Ultrahigh energy density Li-ion batteries based on cathodes of 1D metals with –Li–N–B–N– repeating units in α-Li_xBN_2 ($1 \leq x \leq 3$)

Károly Németh[a)]
Physics Department, Illinois Institute of Technology, Chicago, Illinois 60616, USA

(Received 18 June 2014; accepted 21 July 2014; published online 6 August 2014)

Ultrahigh energy density batteries based on α-Li_xBN_2 ($1 \leq x \leq 3$) positive electrode materials are predicted using density functional theory calculations. The utilization of the reversible $LiBN_2 + 2\,Li^+ + 2\,e^- \rightleftharpoons Li_3BN_2$ electrochemical cell reaction leads to a voltage of 3.62 V (vs Li/Li^+), theoretical energy densities of 3251 Wh/kg and 5927 Wh/l, with capacities of 899 mAh/g and 1638 mAh/cm^3, while the cell volume of α-Li_3BN_2 shrinks only 2.8% per two-electron transfer on charge. These values are far superior to the best existing or theoretically designed intercalation or conversion-based positive electrode materials. For comparison, the theoretical energy density of a Li–O_2/peroxide battery is 3450 Wh/kg (including the weight of O_2), that of a Li–S battery is 2600 Wh/kg, that of $Li_3Cr(BO_3)(PO_4)$ (one of the best designer intercalation materials) is 1700 Wh/kg, while already commercialized $LiCoO_2$ allows for 568 Wh/kg. α-Li_3BN_2 is also known as a good Li-ion conductor with experimentally observed 3 mS/cm ionic conductivity and 78 kJ/mol ($\approx$0.8 eV) activation energy of conduction. The attractive features of α-Li_xBN_2 ($1 \leq x \leq 3$) are based on a crystal lattice of 1D conjugated polymers with –Li–N–B–N– repeating units. When some of the Li is deintercalated from α-Li_3BN_2 the crystal becomes a metallic electron conductor, based on the underlying 1D conjugated π electron system. Thus, α-Li_xBN_2 ($1 \leq x \leq 3$) represents a new type of 1D conjugated polymers with significant potential for energy storage and other applications.
 [http://dx.doi.org/10.1063/1.4891868]

I. INTRODUCTION

There is a quest for materials that would allow for storing large amounts of energy per unit weight and volume and can be utilized as electroactive species in electrochemical energy storage devices. These materials typically serve as part of the positive electrode of batteries while negative electrodes may be composed of bulk metals, such as Li, Na, Mg, Al, etc., or as electrically and ionically conductive composite materials containing these metals. The driving force of the discharge process in batteries is the chemical potential difference of electrons and mobile cations in the positive and negative electrodes manifesting as voltage between the current collectors. Main stream battery research focuses on improving Li-ion batteries that are based on positive electrode materials capable of intercalating/deintercalating Li^+ ions during the charge/discharge processes. The most promising Li^+ ion intercalating materials involve layered oxides $LiMO_2$, spinels LiM_2O_4, polyanionic compounds such as olivine compounds $LiMPO_4$, silicate compounds Li_2MSiO_4, tavorites $LiMPO_4F$, and borates $LiMBO_3$, where M denotes a transition metal atom, usually Co, Mn, Fe, Cr, V, Ni, and Ti, sometimes M=Al may also occur.[1,2] There are also conversion based cell reactions when the mobile cation does not intercalate into a host crystal but forms separate crystals with anions taken out from the host material. Examples of conversion-based batteries include the reactions of Li with S,[3] $(CF)_x$,[4] and FeF_3.[5] Representative theoretical gravimetric energy densities of these batteries are 2600 Wh/kg for Li–S,[3] 1950 Wh/kg for Li–FeF_3,[5] 1700 Wh/kg for $Li_3Cr(BO_3)(PO_4)$,[6] and 568 Wh/kg for $LiCoO_2$.[7] In practice, these values are far smaller due to additional materials that are needed for practical implementations of the corresponding electrochemistries. For example, best realized Li–S batteries allow for 300-500 Wh/kg[3] which is still significantly better than that of commercially available batteries (130–200 Wh/kg, based on $LiMO_2$). For intercalation-based cathode materials there is typically a factor of 3–4 difference between the theoretical and practical energy density values. Research is also conducted on metal-air type batteries that have extremely large theoretical energy densities. A rechargeable Li–O_2/peroxide battery has a theoretical energy density of 11 kWh/kg when O_2 is taken from air, or 3450 Wh/kg when O_2 is carried within the battery.[8] However, the realization of rechargeable metal-air batteries appears the most difficult endeavor among all battery development directions.[8,9]

As the ideal electrode material is both a good electron and ion conductor, electrically conducting quasi 1D polymers have also been subject of battery research.[10] These polymers are based on conjugated π-electron systems, such as polyacetylene, polyaniline, polypyrrole, polythiophene, etc. Perhaps, the best performing polymer of this kind is polyaniline. Polyaniline cathodes and lithium anodes can achieve a theoretical energy density of 340 Wh/kg (in reference to the weight of the electroactive materials) at a voltage of 3.65 V[10] using $LiClO_4$ electrolyte where the ClO_4^- ions play the role of dopant of the conductive polymer in the charged state of a supercapacitor type device whereby the polymer carries

a)nemeth@agni.phys.iit.edu

positive charges. Poly(sulfur nitride) (also called polythiazyl), the first known example of a polymeric conductor that is also superconductor below 0.3 K, has also been tested in battery applications, achieving 90 Wh/kg theoretical energy density.[11] However, due to its explosivity when heated to 240 °C, or due to mechanical impact or electrical ark[12] its application is rendered unsafe in batteries. Conjugated 1D polymers occur in many other materials, especially in coordination polymers, such as CuCN, AgCN, AuCN, or ternary acetylides.[13,14]

α-Li_3BN_2 (space group $P4_2/mnm$[15]), a derivative of hexagonal boron nitride (h-BN) that forms when reacting h-BN with molten Li_3N,[16–18] provides an interesting example of 1D conjugated polymers with –Li–N–B–N– repeating units. The –N–B–N– part of the –Li–N–B–N– repeating unit is the dinitridoborate anion, BN_2^{3-}, thus each repeating unit –Li–N–B–N– carries two negative charge. The two negative charge of the –Li–N–B–N– repeating unit is counterbalanced by two Li^+ ions per formula unit, located between sheets of the polymeric strands as shown in Fig. 1(a). This layered structure strongly resembles to that seen, for example, in layered oxide materials used in Li ion batteries.

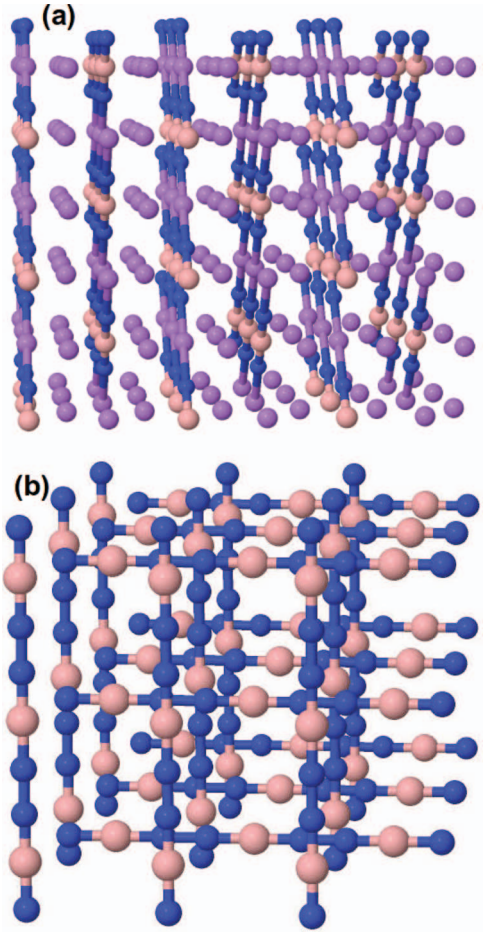

FIG. 1. The structure of α-Li_3BN_2 (panel (a)) and that of the predicted derivative α-BN_2 compound (panel (b)), in 3 × 3 × 3 supercells. Color code: N – blue, Li – violet, B – magenta. Linear polymers with –Li–N–B–N– repeating units are present in α-Li_3BN_2, where they form layers. Between the layers, additional Li ions take place tetrahedrally coordinating to nearest N atoms. These latter Li ions are predicted to be deintercalatable without the collapse of the rest of the crystal. When all Li-s are deintercalated, structures like α-BN_2 may form.

In each polymer-containing layer, the polymer strands are running parallel with half the length of the repeating unit shifted relative to the neighboring strand so that each B atom will have a Li neighbor in the neighboring strand. Nearest neighbor polymer-containing layers are rotated by 90° relative to each other and are placed such that in the direction perpendicular to the layers each B atom will have a Li neighbor again. As a result, in α-Li_3BN_2 each B atom is octahedrally coordinated to neighboring Li atoms of polymeric strands, and vice versa for the Li-atoms in the polymers. The distance between Li atoms and their nearest N neighbors is 1.95 Å in the polymers, which counts as a strong coordinative Li-N bond. The Li atoms between the polymer-containing layers are coordinated tetrahedrally to four nearest N atoms of polymers at a distance of 2.12 Å. α-Li_3BN_2 contains one two-coordinated Li atom (in the polymer) and two four-coordinated Li atoms (between the polymeric layers) per formula unit. These Li atoms will be referred to as Li(2N) and Li(4N), respectively, in the following.

There are two other known phases of Li_3BN_2 besides the α one. In the closely related other phase with space group $I4_1/amd$,[16,19] the polymer strands are running parallel in the layers without any relative shift, so B atoms have B neighbors in neighboring strands (and vice versa for Li). In the neighboring layers, B atoms have one B and one Li neighbor. This results in an asymmetric force-field and bends the polymer strands by 7°–8° at each B atom and by 16° at each Li(2N) atom. The third known phase of Li_3BN_2 is the monoclinic one[20] (space group $P2_1/c$, also called the beta phase), this phase does not contain linear chains of –Li–N–B–N– repeating units, all Li-s are of Li(4N) type.

The Li-ion conductivities of the α, $I4_1/amd$, and monoclinic phases have been measured at T = 400 K temperature, nearly 30 years ago, and have been found to be 3, 6, and 6 mS/cm with activation energies of 78, 64, and 64 kJ/mol, respectively.[16,20,21] These Li ion conductivities count as good and are comparable to that of other Li-ion battery intercalation cathode materials. For example, $LiCoO_2$ has Li-ion conduction and intercalation/deintercalation activation energies of 37–69 kJ/mol.[22] Despite the analogies of the structure of Li_3BN_2 with known Li-ion battery cathode materials and to its good ionic conductivity, to the best of our knowledge, Li_3BN_2 has not been investigated yet as a positive electrode electroactive material, it has only been considered as Li-ion conductor[23] or as component of conversion based anode[24] materials. Li_3BN_2 is an attractive candidate for intercalation-based positive electrode electroactive material, as it is built only of light elements of the second row of the periodic table, therefore it is much lighter per formula unit than the typical intercalation cathode materials that contain heavy transition metals. This low weight per formula unit may result in high gravimetric energy density, when the corresponding cell reaction is energetic enough. Therefore, the present study focuses on theoretical calculations regarding the potential application of Li_3BN_2 phases as positive electrode materials in batteries. While α-Li_3BN_2 has already been proposed for use as a positive electrode material by the present author in a recent

publication[25] and some of its most important characteristics has been briefly discussed there, the present work provides a comprehensive theoretical analysis of the system.

The most important criteria for the design of efficient intercalation cathode materials include an as high as possible intercalation potential (relative to the anode applied),[6,26–28] high capacity, i.e., high concentration of mobile cations,[29] high cation mobility,[30,31] good electric conductivity,[22] structural stability, and an as small as possible volume change during the cycling of the battery.[6] To the best of the present author's knowledge, all of the existing materials designs for Li-ion intercalation cathode materials are based on transition metal compounds and it is the transition metal that changes its oxidation number during the cycling of the battery. The present study significantly differs from these approaches in as much as it will be a light atom, namely, nitrogen, in the proposed battery material that changes its oxidation number during the cycling of the battery, and no transition metal will be involved. The theoretical methodology that will be used to study this proposed material, Li_3BN_2, is a standard one that has been used in many of the cathode material investigations.

II. METHODOLOGY

In the Li_3BN_2 phase with $I4_1/amd$ space group symmetry, the –Li–N–B–N– polymers are bent and the collapse of the polymers can be expected when Li ions are deintercalated. The monoclinic phase has no polymers and it appears difficult to define a stable structure after the deintercalation of Li-ions. Therefore, the following computations will focus on the electrochemical properties of α-Li_3BN_2, where stable crystal structure of –Li–N–B–N– polymers can be expected even after the deintercalation of the Li-ions from the Li(4N) positions. As there are two Li(4N) atoms per formula unit in α-Li_3BN_2, the proposed cell reaction is the following:

$$LiBN_2 + 2Li^+ + 2e^- \rightleftharpoons Li_3BN_2. \quad (1)$$

The intercalation electrode potential of the cell reaction, relative to the anode potential, can be calculated from the Gibbs free energy of the reaction, ΔG, expressed in eV and divided by the number of electrons transferred. If the entropy contribution is small (volume change is negligible), ΔG can be approximated as the change of electronic energy, ΔE during the reaction.[6,26,27] In the case of the above reaction, ΔE can be expressed as

$$\Delta E = E(Li_3BN_2) - E(LiBN_2) - 2E(Li), \quad (2)$$

where $E(Li_3BN_2)$, $E(LiBN_2)$, and E(Li) refer to the electronic energy of the corresponding crystals per formula unit, for α-Li_3BN_2, for the derivative α-$LiBN_2$ obtained after deintercalating all Li(4N)-s and for bulk metallic Lithium, respectively. The open circuit voltage of the above cell reaction will be $U = -\Delta E/2$, as two electrons have been transferred. This U voltage is identical with the intercalation electrode potential of $LiBN_2/LiBN_2^{2-}$ relative to the Li/Li^+ electrode.

The electronic energy change during the cell reaction is often calculated using the density functional theory (DFT)(GGA)+U method,[32] in order to account for problems of DFT in predicting properties of transition metal compounds.[6,26,27] Since there is no transition metal in the present cell reaction, a simpler approach may be followed here, using the PBEsol[33,34] exchange-correlation functional to calculate electronic energies and optimum crystal structures. The performance of the PBEsol functional on crystals as compared to other exchange correlation functionals is assessed, for example, in Ref. 35, as of today, the PBEsol functional appears one of the best choices for crystal geometries, energies, and band-structures for systems composed of light atoms, such as those in Li_3BN_2. The Quantum-Espresso[36] code is used with ultrasoft pseudopotentials (as provided with the code) in a plane-wave basis with 50 Ry wavefunction cutoff. A 10 × 10 × 10 k-space grid is used to discretize the electronic bands (unless otherwise noted). Optimum crystal structures have less than 1.d−4 Ry/bohr residual forces with residual pressure of less than 1 kbar on the unit cells. Electronic energies refer to optimum structures unless otherwise noted. The methodology has been validated on experimental data of lattice parameters and enthalpies of formation of α-Li_3BN_2, Li_3N, and h-BN. Enthalpies of formations were estimated as the change of electronic energy during the formation of the compounds from the corresponding elements at T = 0 K, i.e., from crystalline Li and B and N_2 gas.

Experimental lattice parameters of α-Li_3BN_2 are a = b = 4.6435 Å and c = 5.2592 Å,[15] while calculated ones are 4.6019 and 5.1317 Å, respectively, an agreement within 1.0% and 2.5%, respectively. For Li_3N (with a 6 × 6 × 6 k-space), experimental lattice parameters are a = b = 3.6373 Å and c = 3.8703 Å,[37] while calculated ones are a = b = 3.5549 Å and c = 3.8088 Å, an agreement within 2.3% and 1.6%, respectively. For h-BN (with a 6 × 6 × 6 k-space), a = b = 2.5039 Å and c = 6.6612 Å,[38] while calculated ones are a = b = 2.5032 Å and c = 7.0191 Å, respectively, an agreement within 0.03% and 5.3%, respectively; note that the latter discrepancy is due to the known inaccuracy of the PBEsol functional to describe intermolecular interaction.

The experimental standard enthalpy of formation of α-Li_3BN_2 is −534.5 (±16.7) kJ/mol,[39] the calculated one is −512.0 kJ/mol (4.2% difference). For Li_3N, the corresponding values are −164.5 kJ/mol[40] and −161.5 kJ/mol, respectively (1.9% difference). For h-BN, the experimental value is −250.9 kJ/mol,[41] the calculated one is −260.9 kJ/mol (3.9% difference).

III. RESULTS AND DISCUSSION

The cell reaction in Eq. (1) assumes the existence of the BN_2^- anion, the oxidized form of BN_2^{3-}. While BN_2^{3-} has been known for decades, no compounds with its oxidized form, BN_2^- are known, to the best of the present author's knowledge.

Resonance structures of the BN_2^{3-} anion and related anions are discussed in Fig. 1 of Ref. 42. Analogously, resonance structures of its oxidized form, BN_2^-, have been depicted in the present work in Fig. 2. It appears that on the basis of the resonance structures the existence of the oxidized form, BN_2^- is possible, especially when it is stabilized in linear chains with repeating BN_2^- and Li^+ ions, being part of a linear conjugated π-electron system. The oxidation of BN_2^{3-}

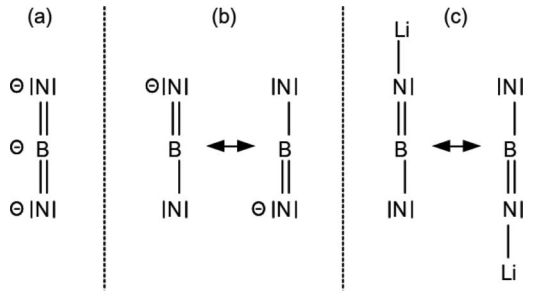

FIG. 2. Resonance structures of the dinitridoborate, BN_2^{3-} anion (panel (a)) and its oxidized version, BN_2^- (panel (b)), as well as that of the –Li–N–B–N– repeating unit in $LiBN_2$.

can also be viewed as if BN_2^{3-} would be a way of storing a nitride ion, N^{3-} absorbed to a neutral diatomic BN molecule and allowing for the electrochemistry of the N^{3-} ion within this complex. The N^{3-} ion represents an oxidation state of N as in ammonia (NH_3) or in lithium nitride (Li_3N), while the oxidized form N^{2-} is familiar from hydrazine (N_2H_4) and the further oxidized form N^- is known from lithium-diazenide (Li_2N_2).[43] The Li_3BN_2 molecule may be viewed as a combination of half of a Li_2N_2 and half of a hydrazine-like Li_4N_2 through a B atom, whereby the B binds with a double bond to the diazenide-type N and with a single bond to the hydrazine-type N. Albeit oxidized forms of the BN_2^{3-} ion, such as BN_2^{2-} and BN_2^- have not been reported in the literature yet, there is recent indirect evidence about the existence of BN_2^{2-} in Na_2BN_2 obtained during thermogravimetric analysis of the thermolysis of Na_2KBN_2, after the evaporation of all K in a well separable step.[44]

The calculated intercalation electrode potential of the cell reaction in Eq. (1) is $U(LiBN_2/Li_3BN_2) = 3.62$ V, relative to a Li/Li^+ electrode. The energy of the cell reaction is $\Delta E(LiBN_2/Li_3BN_2) = 7.24$ eV per two electron transfer. The mass-density of α-Li_3BN_2 is $\rho(Li_3BN_2) = 1.823$ g/cm^3. The gravimetric energy density is $\rho_{EG}(Li_3BN_2) = 3251$ Wh/kg, the volumetric energy density is $\rho_{EV}(Li_3BN_2) = 5927$ Wh/l. The gravimetric capacity, i.e., the concentration of de/re-intercalatable Li, is $\rho_{CG}(Li_3BN_2) = 899$ mAh/g, the volumetric one is $\rho_{CV}(Li_3BN_2) = 1638$ mAh/cm^3 . The cell volume of α-Li_3BN_2 changes only by 2.8% per two-electron transfer (shrinks during deintercalation). Calculated lattice parameters of α-Li_3BN_2 are a = b = 4.6019 and c = 5.1317 Å, while for the deintercalated α-$LiBN_2$ they are a = b = 4.5460 and c = 4.9613 Å, note that each unit cell contains two formula units of material. The calculated characteristic nearest atomic distances barely change during the deintercalation: the symmetric Li(2N)–N, Li(4N)–N, and B–N bond lengths are 1.912, 2.092, and 1.343 Å in α-Li_3BN_2, they are 1.932, 2.062, and 1.337 Å in α-Li_2BN_2 and 1.888, none and 1.327 Å in α-$LiBN_2$, respectively.

The energy density and capacity values of α-Li_3BN_2 are far superior to those of other known or designer cathode materials, listed in Sec. I. For a brief comparison, representative theoretical gravimetric energy densities of these other cell reactions are 2600 Wh/kg for Li–S (conversion-based),[3] 1950 Wh/kg for Li–FeF_3 (conversion-based),[5] 1700 Wh/kg for $Li_3Cr(BO_3)(PO_4)$ (intercalation-based),[6] and 568 Wh/kg for $LiCoO_2$ (intercalation-based).[7] In fact, the theoretical energy density of α-Li_3BN_2, 3251 Wh/kg, is very close (within 6%) to that of a Li–O_2/peroxide battery, 3450 Wh/kg, when O_2 is carried within the battery.[8]

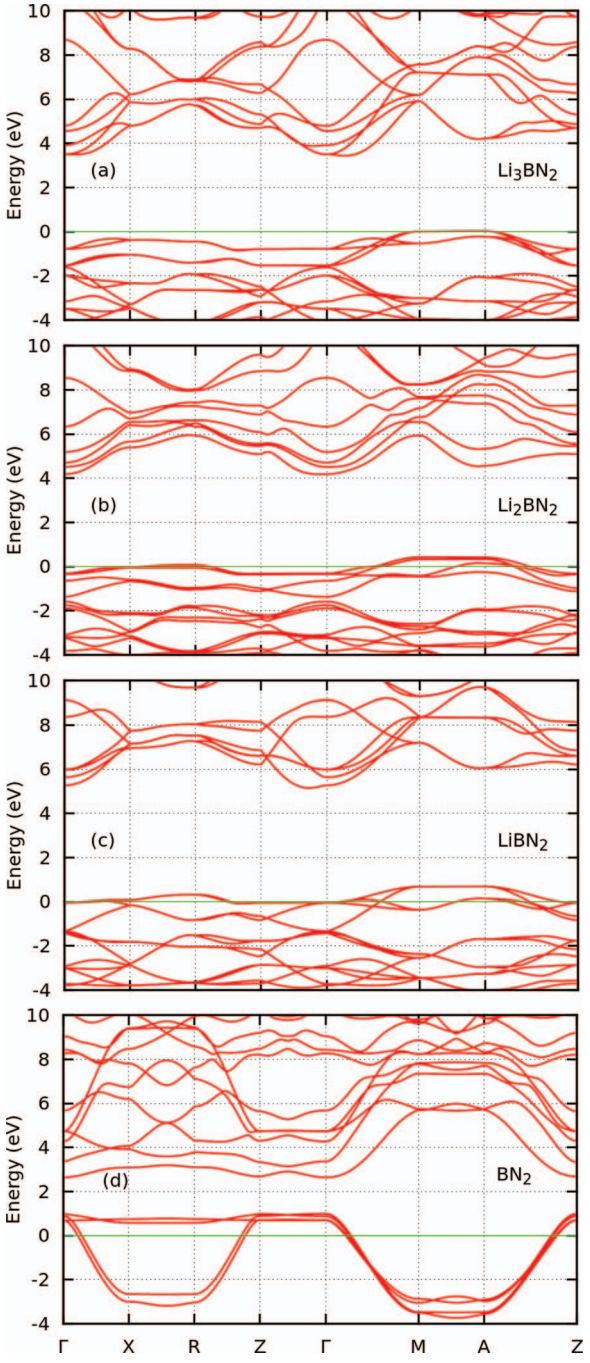

FIG. 3. (a)-(d) Bandstructures of compounds obtained by gradual extraction of Li from α-Li_3BN_2. The origin of the energy scale is set to the Fermi energy for each compound.

Fig. 3 shows the electronic bands in α-Li_3BN_2 and in its gradually delithiated versions, Li_2BN_2, $LiBN_2$, and BN_2. Note that the Li in the –Li–N–B–N– chains is extracted only in the last step, in order to preserve the polymeric skeleton of the crystal. Many possible structures may form after the complete extraction of the Li. From the many variants, the depicted structure of BN_2 in Fig. 1 (panel (b)) appears to be

TABLE I. Binding energies, ε, of Li(2N) and Li(4N) atoms in α-Li_nBN_2 (n ∈ [0,3]) and net charges Q on the various types of atoms. Some charge is lost during the projection of electron density from plane-wave basis into atomic orbital one (Löwdin charges). Binding energies for all systems have been calculated at the relaxed structure obtained with the Li(2N) positions filled, except for ε(Li(2N)) at n = 2 where the optimum structure of n = 3 has been used. ε values are relative to binding energy of Li in crystalline Li.

	ε (eV)		Q/e			
n	Li(2N)	Li(4N)	B	N	Li(2N)	Li(4N)
3	− 3.326	− 3.564	0.00	− 1.04	+0.78	+0.76
2	− 3.817	− 3.664	+0.07	− 0.75	+0.79	+0.78
1	− 4.431	− 4.278	+0.17	− 0.42	+0.79	…
0	…	…	+0.25	− 0.05	…	…

the most analogous one to α-Li_3BN_2 in the sense that linear polymers with –N–B–N– repeating units are preserved and the relative orientation of these polymers is similar to that in α-Li_3BN_2. As indicated by the bandstructures, the delithiation results in metallic systems, as holes are created in the valence band of α-Li_3BN_2 and the Fermi level decreases below the top of the valence band of α-Li_3BN_2 while no bandgap opens. This phenomenon is similar to that observed in the $LiCoO_2$ cathode material which also becomes metallic upon delithiation.[22] Only the α-Li_xBN_2 ($1 \le x \le 3$) systems are suitable for intercalation-based electrodes, as BN_2 has a significantly different cell volume.

The binding energies of Li(2N) and Li(4N) atoms are listed in Table I, they also represent the intercalation potentials of Li-s in the specific positions in the given optimum crystal structures. Except for the completely lithiated crystal, in all other cases the Li(2N)-s are stronger bound than the Li(4N)-s, i.e., the energetically favorable position of the Li ions is in the –Li–N–B–N– chains. This result has been validated also in a 3 × 3 × 3 supercell of $LiBN_2$ (54 formula units, 216 atoms). At the optimum geometry (obtained with all Li-s in Li(2N) positions) a single Li ion has been moved into a tetrahedral Li(4N) position. As a result, the electronic energy of the system increased by ΔE(2N/4N) = 0.83 eV. The Li(2N) filling appears more energetically favored over the Li(4N) one because the planes filled by the –Li–N–B–N– polymers are negatively charged and the electrostatic potential has a minimum for Li^+ ions in these planes, as indicated in Fig. 4.

The experimental value of the activation energy of Li-ion conduction in Li_3BN_2 is 0.81 eV[16] which is close to the above value of ΔE(2N/4N), suggesting that one possible mechanism of Li-ion conduction in Li_xBN_2 ($1 \le x \le 3$) is based on Li^+ jumping between nearby Li(2N) and Li(4N) sites, with the Li(4N) site being the transition state. This Li ion conduction mechanism is also suggested by the plane averaged electrostatic potential distribution in Fig. 4: Li ions between the polymeric planes are tetrahedrally coordinated (Li(4N) sites) and sit on top of the electrostatic potential maxima, i.e., in transition states of the plane averaged electrostatic potential, and are expected to fall into nearby minima of the plane averaged electrostatic potential within the polymeric planes when Li ion vacancies (empty Li(2N) sites) are available in these planes. The present study investigated other possible mechanisms as well, such as Li(4N) to Li(4N) jumping parallel to –Li–N–B–N– planes or perpendicular to these planes. The initial guesses for the transition states were selected such that the Li ions in the Li(4N) positions were shifted halfway towards one of the nearest neighbor Li(4N) sites then these approximate transition states were relaxed. The shifted Li ions induced too short atomic distances and the subsequent relaxations generated large geometric changes and large increase in the electronic energy (2 eV and above) of the simulation cell.

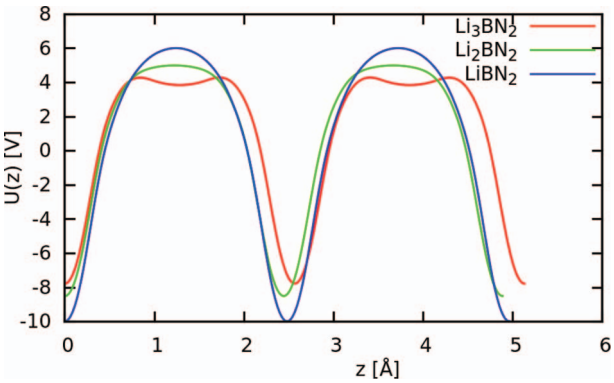

FIG. 4. The plane-averaged electrostatic potential, U(z) along the z axis (parallel with main crystallographic axis, c) for α-Li_nBN_2, with n = 1, 2, or 3. The minima are located in the planes filled with –Li–N–B–N– polymers. The electrostatic potential attracts Li-ions to fill available Li-vacancies in the –Li–N–B–N– chains, thereby self-repairing –Li–N–B–N– chains during the $Li_3BN_2 \rightarrow LiBN_2 + 2$ Li deintercalation process, i.e., on charging the battery. The layers along the z axis of α-Li_xBN_2 ($1 \le x \le 3$) act as capacitor plates with alternating majority charges.

Partial (Löwdin) charges of the various types of atoms are listed in Table I. Note that the charges do not sum up to the formal charges of the corresponding ions (such as BN_2^{3-} and BN_2^{2-}) since the projection from plane-wave basis into atomic orbitals is incomplete. However, tendencies of atomic charges give an account on how the charge is stored in the various oxidation states of the system. As the oxidation of BN_2^{n-} ($1 \le n \le 3$) goes on with decreasing n and decreasing Li-content, the B atoms become gradually slightly more positively charged while the N atoms become significantly less negatively charged and the charge of the Li-s stays constant. The fact that B has near zero net charge in BN_2^{3-} and in its oxidized forms indicates that B carries significantly more electrons in these ions than it does in h-BN, where the charge of B is ≈ + 0.5. From this analysis it is clear that the reduction/oxidation processes in the Li_xBN_2 ($1 \le x \le 3$) system are mainly associated with the N atoms, in concert with the above mentioned analogies of Li_xBN_2 to various types of molecules with varying oxidation number of the N atom (Li_3N, N_2H_4, Li_2N_2).

The application of the $I4_1$/amd and monoclinic phases as electroactive material is expected to result in large volume changes, albeit at similarly high voltages, as in all cases the BN_2^{3-} ions are oxidized/reduced. As the electrochemical cycling of batteries often causes phase transformations in the electroactive crystals, it can be expected that the use of the $I4_1$/amd and monoclinic phases might result in phase transformation to the α phase whereby minimizing the volume changes of the electroactive material.

Concerning the stability of the oxidized forms of BN_2^{3-}, i.e., that of BN_2^{2-} and BN_2^{-}, there is no experimental evidence yet, except the indirect one mentioned above for the existence of BN_2^{2-} in Na_2BN_2.[44] The thermal decomposition of Na_3BN_2 and Na_2KBN_2 as well as that of Na_2BN_2 leads to elemental alkali metals, h-BN and N_2 at temperatures above 710 and 800 K.[44] It is customary to calculate decomposition voltages of electroactive species, based on the reaction enthalpies of the decomposition processes. These decomposition voltages may significantly differ from actual decomposition voltages as the decomposition process may be kinetically hindered even if it is thermodynamically allowed. Assuming that the decomposition of the α-Li_xBN_2 ($1 \le x \le 3$) materials would result in h-BN, N_2 gas and elemental Li, the calculated decomposition potentials relative to Li/Li^+ are 0.87, −0.48, and −4.63 V for x = 3, 2, and 1, respectively, where the negative sign denotes exotherm decomposition. These voltages indicate that decomposition is thermodynamically allowed at the 3.62 V estimated operating voltage if the partial pressure of N_2 is sufficiently low. The effect of the partial pressure of N_2 on the decomposition voltage is also utilized in N_2 sensors, for example, based on Li_3AlN_2.[45] One way to increase the decomposition potential and thus the stability of α-Li_xBN_2 ($1 \le x \le 3$) is to apply a high enough partial pressure of N_2. This may be possible by coating the α-Li_xBN_2 particles such that N_2 cannot escape.

Another way to increase the decomposition voltage is based on doping. A related material, Li_3N, has a decomposition potential of 0.44 V (vs Li/Li^+) that can be raised to 1.86 V when doped with LiCl to form $Li_9N_2Cl_3$.[46] The principle behind such doping is that the dopant must be of high decomposition voltage (high enthalpy of formation) thus it can raise the enthalpy of formation of the doped system, and the dopant must form a solid solution with the doped material. A particularly attractive choice for dopant is Li_2S.

The proposed α-Li_xBN_2 ($1 \le x \le 3$) and BN_2 also have merits as new conductive polymers based exclusively on Li, B, and N or on B and N, opening up new paths in the field of synthetic metals as well.

One potential objection to the use of boron containing electroactive materials, such as Li_3BN_2, is that boron is not an earth abundant material. However, the known boron resources are sufficiently large to allow for a widespread use of such devices. The proven global boron reserves are 369×10^6 tons of B_2O_3, the total reserves are at 1176×10^6 tons when including the probable possible reserves.[47] These are equivalent to 114×10^6 and 364×10^6 tons of pure boron, respectively. An energy storage device storing 90 kWh energy (useful energy stored in gasoline in a typical car) would require 5 kg boron in 28 kg of Li_3BN_2 (about 15 l volume) using the theoretical specific energy of Li_3BN_2. For 7×10^9 people, this would add up to 35×10^6 tons of boron, about 10% of the estimated total boron reserves.

IV. SUMMARY AND CONCLUSIONS

The present work provides a detailed theoretical analysis on the proposed use of α-Li_xBN_2 ($1 \le x \le 3$) as electroactive species in the positive electrode of electrochemical cells. It is predicted by means of density functional theory calculations, that the application of this material can result in 3.62 V cells (relative to Li/Li^+), a gravimetric energy density of 3251 Wh/kg, a volumetric one of 5927 Wh/l, and gravimetric and volumetric capacities of 899 mAh/g and 1638 mAh/cm^3, respectively, when two Li ions are intercalated per formula unit. The predicted associated volume change is only 2.8% per two-electron transfer. The Li-deintercalated structures are metallic, when sufficient amount of Li is extracted. These predicted properties are far superior to other existing or designer Li-intercalation based battery materials and are even comparable to the theoretical energy density of a Li-O_2/peroxide battery, 3450 Wh/kg, when O_2 is carried within the battery. Furthermore, these materials are also interesting as they are based on novel 1D conjugated π-electron systems representing new conducting polymers.

ACKNOWLEDGMENTS

The author thanks Professor L. Shaw (IIT) for discussions and NERSC (U.S. Department of Energy (DOE) DE-AC02-05CH11231) for the use of computational resources.

[1] B. Xu, D. Qian, Z. Wang, and Y. S. Meng, Mater. Sci. Eng. R **73**, 51 (2012).
[2] B. C. Melot and J.-M. Tarascon, Acc. Chem. Res. **46**, 1226 (2013).
[3] M.-K. Song, Y. Zhang, and E. J. Cairns, Nano Lett. **13**, 5891 (2013).
[4] P. Meduri, H. Chen, J. Xiao, J. J. Martinez, T. Carlson, J.-G. Zhang, and Z. D. Deng, J. Mater. Chem. A **1**, 7866 (2013).
[5] L. Li, F. Meng, and S. Jin, Nano Lett. **12**, 6030 (2012).
[6] G. Hautier, A. Jain, H. Chen, C. Moore, S. P. Ong, and G. Ceder, J. Mater. Chem. **21**, 17147 (2011).
[7] M. M. Thackeray *et al.*, "Lithium-oxygen (air) electrochemical cells and batteries," U.S. patent 8,313,721 (20 November 2012).
[8] J. Christensen, P. Albertus, R. S. Sanchez-Carrera, T. Lohmann, B. Kozinsky, R. Liedtke, J. Ahmed, and A. Kojic, J. Electrochem. Soc. **159**, R1 (2012).
[9] K. Németh and G. Srajer, RSC Adv. **4**, 1879 (2014).
[10] P. Novák, K. Müller, K. Santhanam, and O. Haas, Chem. Rev. **97**, 207 (1997).
[11] R. Archer, *Inorganic and Organometallic Polymers*, Special Topics in Inorganic Chemistry Vol. 4 (Wiley, 2004).
[12] D. Downs, H. Fair, and Z. Iqbal, "Electric initiator containing polymeric sulfur nitride," U.S. patent 4,206,705 (10 June 1980).
[13] U. Ruschewitz, Z. Anorg. Allg. Chem. **632**, 705 (2006).
[14] J. Z. Terdik, K. Németh, K. C. Harkay, J. H. Terry, Jr., L. Spentzouris, D. Velázquez, R. Rosenberg, and G. Srajer, Phys. Rev. B **86**, 035142 (2012).
[15] K. Cenzual, L. M. Gelato, M. Penzo, and E. Parthé, Acta Crystallogr. B **47**, 433 (1991).
[16] H. Yamane, S. Kikkawa, and M. Koizumi, J. Solid State Chem. **71**, 1 (1987).
[17] R. DeVries and J. Fleischer, Mater. Res. Bull. **4**, 433 (1969).
[18] J. Goubeau and W. Anselment, Z. Anorg. Allg. Chem. **310**, 248 (1961).
[19] F. Pinkerton and J. Herbst, J. Appl. Phys. **99**, 113523 (2006).
[20] H. Yamane, S. Kikkawa, H. Horiuchi, and M. Koizumi, J. Solid State Chem. **65**, 6 (1986).
[21] H. Yamane, S. Kikkawa, and M. Koizumi, J. Power Sources **20**, 311 (1987).
[22] X.-Y. Qiu, Q.-C. Zhuang, Q.-Q. Zhang, R. Cao, P.-Z. Ying, Y.-H. Qiang, and S.-G. Sun, Phys. Chem. Chem. Phys. **14**, 2617 (2012).
[23] F. Waechter and R. Nesper, "Coating and lithiation of inorganic oxidants by reaction with lithiated reductants," U.S. patent application 13/724,748 (27 June 2013).
[24] T. H. Mason, X. Liu, J. Hong, J. Graetz, and E. Majzoub, J. Phys. Chem. C **115**, 16681 (2011).
[25] K. Németh, Int. J. Quantum Chem. **114**, 1031 (2014).
[26] F. Zhou, M. Cococcioni, K. Kang, and G. Ceder, Electrochem. Commun. **6**, 1144 (2004).
[27] A. Jain, G. Hautier, S. P. Ong, C. J. Moore, C. C. Fischer, K. A. Persson, and G. Ceder, Phys. Rev. B **84**, 045115 (2011).

[28]T. Mueller, G. Hautier, A. Jain, and G. Ceder, Chem. Mater. **23**, 3854 (2011).
[29]K. Kang, Y. S. Meng, J. Breger, C. P. Grey, and G. Ceder, Science **311**, 977 (2006).
[30]B. Kang and G. Ceder, Nature (London) **458**, 190 (2009).
[31]D. M. Duong, V. A. Dinh, and T. Ohno, Appl. Phys. Exp. **6**, 115801 (2013).
[32]V. I. Anisimov, J. Zaanen, and O. K. Andersen, Phys. Rev. B **44**, 943 (1991).
[33]J. P. Perdew, K. Burke, and M. Ernzerhof, Phys. Rev. Lett. **77**, 3865 (1996).
[34]J. P. Perdew, A. Ruzsinszky, G. I. Csonka, O. A. Vydrov, G. E. Scuseria, L. A. Constantin, X. Zhou, and K. Burke, Phys. Rev. Lett. **100**, 136406 (2008).
[35]L. Schimka, J. Harl, and G. Kresse, J. Chem. Phys. **134**, 024116 (2011).
[36]P. Giannozzi, S. Baroni, N. Bonini, M. Calandra, R. Car, C. Cavazzoni, D. Ceresoli, G. L. Chiarotti, M. Cococcioni, I. Dabo *et al.*, J. Phys.: Condens. Matter **21**, 395502 (2009); see http://www.quantum-espresso.org for a general description of the Quantum Espresso software package.
[37]A. Huq, J. W. Richardson, E. R. Maxey, D. Chandra, and W.-M. Chien, J. Alloys Comp. **436**, 256 (2007).
[38]R. S. Pease, Acta Crystallogr. **5**, 356 (1952).
[39]J. McHale, A. Navrotsky, and F. DiSalvo, Chem. Mater. **11**, 1148 (1999).
[40]*NIST-JANAF Themochemical Tables*, 4th ed., Journal of Physical and Chemical Reference Data: Monograph Issue 9, edited by M. W. Chase Jr. (American Chemical Society and the American Institute of Physics, Washington DC, 1998) [Online; accessed 2-May-2013], available at: http://webbook.nist.gov/chemistry/.
[41]S. S. Wise, J. L. Margrave, H. M. Feder, and W. N. Hubbard, J. Phys. Chem. **70**, 7 (1966).
[42]B. Blaschkowski, Ph.D. thesis, Universität Tübingen, Tübingen, 2003; available at: http://tobias-lib.uni-tuebingen.de/volltexte/2003/882.
[43]S. B. Schneider, R. Frankovsky, and W. Schnick, Angew. Chem. **124**, 1909 (2012).
[44]C. Koz, S. Acar, Y. Prots, P. Höhn, and M. Somer, Z. Anorg. Allg. Chem. **640**, 279 (2014).
[45]M. Bhamra and D. Fray, J. Mater. Sci. **30**, 5381 (1995).
[46]A. Rabenau, Solid State Ionics **6**, 277 (1982).
[47]*Eti Maden Turkish Boron Mines* [Online; accessed 19-July-2014], available at: http://en.etimaden.gov.tr/about-boron-62s.htm.